Durability of Thermal Barrier Coatings in a High Heat Flux Environment

William J. Brindley and James A. Nesbitt
National Aeronautics and Space Administration
Lewis Research Center
Cleveland, Ohio 44135

Introduction

Thermal shock is a significant factor in the limited service life of SSME high pressure, fuel turbopump (HPFTP) turbine blades [1]. Addition of advanced thermal barrier coatings (TBCs) to the blades could serve to dampen the thermal shock, thereby increasing the life of the blades. However, testing and use of TBCs to date has been performed primarily under moderate heat flux conditions which are typical of aircraft turbines [2,3]. Only limited testing has been conducted that addresses high heat flux and severe thermal shock conditions [4,5]. Therefore, it is not clear if TBCs can survive severe thermal shocks or provide adeqate thermal shock protection to the HPFTP turbine blades. The purpose of this work was to experimentally evaluate the potential durability and protective capability of a variety of advanced TBCs in a cyclic thermal shock environment. A secondary goal of the work was to identify significant parameters affecting TBC life during high heat flux testing. Parameters investigated include top coat [1] thickness, bond coat thickness, substrate type, and substrate geometry. Complementary work performed to evaluate the thermal benefit achieved through the use of TBCs is reported in a companion paper [6].

Experimental

The intent of the first portion of the work was to examine the performance of TBCs of various bond coat and top coat compositions and application techniques in a thermal shock environment. These factors were examined by testing advanced TBCs purchased from 12 vendors in addition to testing coatings applied at NASA-LeRC and NASA-MSFC. Each coating type was applied to two 0.9cm diameter MAR-M 246+Hf tubes and two 0.9cm diameter MAR-M 246+Hf rods by all vendors. The nominal top coat thickness was 0.013cm and the nominal bond coat thickness was 0.010cm for all specimens. Twenty one different coatings were supplied and tested. A summary of the nominal compositions and application techniques of the various top coatings supplied is given in Table 1. The chemistries and application techniques for each of the vendors are

[1] State-of-the-art TBCs, developed primarily for aircraft turbine engines, usually consist of two layers. The outermost layer, or top coat, is an insulating material, generally a ceramic. The innermost layer, or bond coat, is generally an oxidation resistant metallic layer that promotes bonding of the top coat to the substrate. See figure 2 for an example.

also listed in Figures 3 through 6. The thermal shock test environment was developed through the use of a 6450 newton (1450 pound) thrust hydrogen-oxygen rocket engine. The engine used was capable of operating at chamber pressures up to 4.14 MPa (600 psi) and hydrogen rich oxygen to fuel mass ratios (O/F) of 1.0 to 8.0. The engine is theoretically capable of gas temperatures of 1000C to 3220C at the 2.07 MPa (300 psi) chamber pressure used in this study.

Preliminary testing was conducted to establish the operating characteristics of the rocket engine as well as establish meaningful operating parameters for TBC testing. Operating characteristics of interest included temperature uniformity, sample temperature reproducibility and chamber pressure reproducibility. Sample substrate temperature reproducibility, as measured via a TBC coated, thermocoupled specimen, was approximately 5%. The chamber pressure repeatibility was approximately 3%.

Temperature uniformity was examined using temperature indicating paints on tungsten rods at each of the 5 specimen positions in the test specimen holder (figure 1). The indicating paint results led to the use of only the second position to assure reasonable temperature uniformity across the sample (figure 1).

The testing cycle devised from preliminary testing on both tubes and rods included a nominal 1 second heating cycle at a chamber pressure of 2.07 MPa (300 psi) followed by a 30 second gaseous nitrogen quench. The tube specimens were tested at an O/F of 1.3 for up to 20 cycles or until failure, where failure was defined as the initiation of spallation and/or substrate melting. Testing on specimens that survived 20 cycles was continued at an O/F of 1.4 for up to an additional 20 cycles. Testing was continued at an O/F of 1.5 until failure for samples that survived 40 cycles.

The rod specimens were tested at an O/F of 1.4 for up to 20 cycles or until failure. Samples that survived 20 cycles were tested for additional cycles at an O/F of 1.5 until failure.

Gas temperatures at the test position (figure 1) were estimated by extrapolating from the gas temperature measurements of ref. 6. The estimated temperatures are 1750C for an O/F of 1.3, 1950C for an O/F of 1.4 and 2100C for an O/F of 1.5. These temperatures are in excess of the calculated adiabatic gas temperatures for the O/Fs used. The thermal analysis in ref. 6 suggests that coating surface temperatures are within 90-95% of the gas temperatures 0.2-0.4 seconds after ignition. The thermal analysis in ref. 6 also suggests that the initial heat flux in the test rocket engine is similar to that in the HPFTP during start-up of the SSME. Therefore, the tests provided a qualitative assessment of the protective capabilities of TBCs in a high heat flux environment indicative of the start-up thermal transient in the HPFTP.

TBC coated substrate temperature measurements, made at the bond

coat/substrate interface during preliminary testing, indicate maximum substrate tempertures of from 800C to 1200C for O/Fs from 1.2 to 1.5, respectively. Substrate heating rates estimated from the substrate temperature measurements were 750°C/s to 1300°C/s for O/Fs of 1.2 to 1.5.

The testing scheme included increasing the O/F at regular intervals for two reasons. First, by testing in this manner it was possible to both qualitatively rank the lives of the various coatings and to examine the upper temperature limit of the coatings durability. Second, this progressive testing scheme shortened the lives of the best samples to an experimentally practical number of cycles.

Post test analysis of the failed coatings was conducted by optical microscopy and scanning electron microscopy. The analysis allowed comparison among the coating failures observed in this study as well as allowing comparisons to coating failures observed in other types of testing.

The effect of ceramic top coat thickness, bond coat thickness, substrate geometry and substrate composition were examined using in-house, plasma spray coated specimens. The specific sample parameters employed are listed as the independent variables in figures 9a through 9d. The testing conditions for these samples were an O/F of 1.2 for nominally 1 second at a chamber pressure of 2.07 MPa (300 psi) followed by a 30 second gaseous nitrogen quench. The gas temperature at an O/F of 1.2 was estimated to be 1550C.

Results and Discussion

The bar charts in figures 3-6 summarize the results of the cyclic testing of the vendor samples and the NASA LeRC samples. Included in the sample labels on these figures are the nominal top coat compositions and the application techniques. The data in figures 3 and 4 are arranged from left to right in ascending order of the "average"[1] life for each coating. The metal/ZrO_2 composite top coat specimens were tested at O/Fs lower than the standard testing scheme. Both types of metal/ZrO_2 coatings survived 5 cycles at an O/F=1.0 but melted on the first cycle at an O/F of 1.2. Consequently, these results were not included in the results reported for the vendor coatings.

Figures 3 and 4 are compilations of the data for all tubes tested. Figure 3 shows the cyclic life of the tubes to the first observation of coating spallation. The "average" life to the first observation of spallation for the tubes, shown on Figure 3 as a dashed horizontal line, was 5.5 cycles. The minimum life exhibited by any coating was 1

[1] The "average" life, with respect to figures 3-6, is a convienient system but is not rigorously correct since the O/F ratio was changed after every 20 cycles.

cycle and the longest life was 36 cycles. It should be noted that the disparity between the longest and shortest lives would be even greater than indicated if the O/F was not increased every 20 cycles.

Figure 4 shows the cyclic life of the tubes when failure was defined as substrate melting. Note that not all tubes were tested to failure. Some of the tubes were tested only to the first observed coating spallation to facilitate post-test examination of the spalled region. Samples not tested to failure are marked with arrows in figure 4. The average life to substrate melting was 7.0 cycles. The shortest life exhibited by any coating was 1 cycle and the longest life to failure was 42 cycles.

The same five coatings exhibited the longest lives, in terms of average life, for both cycles to first observed spallation and cycles to substrate melting. Three of the five coatings are PS ZrO_2 compositions and the other two are EB-PVD ZrO_2 coatings. It is interesting to note that the replicate specimen of the coating exhibiting the longest life for a single sample, the vendor 3 EB-PVD coated sample, had only average life. This result suggests that EB-PVD coatings have the potential for long lives but can also suffer from reproducibility problems. Plasma sprayed coatings demonstrate the potential for long life (NASA-LeRC coating), but can also exhibit reproducibility problems (vendor 5 coating data in figures 3 and 4).

Figures 5 and 6 show the lives of coated rods to the first observation of spallation and to substrate melting, respectively. The data in figures 5 and 6 are arranged in ascending order of the average life for each coating. Comparison of these charts to those for the tubes (Figures 3 and 4) indicates that the coating life for both tubes and rods follow approximately the same ranking. However, the rods exhibited slightly longer average coating lives in spite of the more severe heating cycle (higher initial O/F) relative to the tubes. This difference in life is apparently due to the difference in the substrate geometry and will be addressed later in the paper. The average life to the first observed spallation for the rods was 8.0 cycles. The average life to substrate melting for the rods was 9.9 cycles. The average lives are denoted by the horizontal dashed lines in figures 5 and 6.

Three of the tube coatings exhibiting the longest lives in terms of average life are among the 5 rod coatings with the longest lives. The NASA-LeRC plasma spray coating, vendor 4 plasma spray coating and vendor 1 EB-PVD coating are among the 5 coatings exhibiting the longest lives regardless of the failure criterion used or the substrate geometry.

It is apparent for figures 3-6 that coatings of the same composition and nominally the same application technique exhibit widely different lives (compare vendor 9 coating life with the NASA-LeRC coatings). The disparity in life apparently results from differences in processing

among the various coating suppliers. Thus, processing plays an important role in determining the life of a coating.

Figures 7 and 8 are micrographs of the failure surfaces of selected test specimens. Figure 7a is a SEM micrograph of the NASA-LeRC plasma sprayed Y_2O_3 stabilized ZrO_2 coating and is typical of the plasma sprayed ZrO_2 coatings examined in this study. Dark areas in the micrograph are NiCrAlY bond coat and the light areas are ZrO_2 top coat. The surface appearance of the ZrO_2 areas in the spalled region is consistent with delamination cracking along plasma spray splat boundaries. This is similar to the appearance of ZrO_2 coatings tested in burner rigs and furnaces [2].

Figure 7b is a cross sectional view of a spalled region in a NASA-LeRC sample tested to spallation. The spalled surface can be described as a thin layer of ceramic adhering to the bond coat with bond coat asperities occasionally protruding from the ceramic, similar to coating failures observed after burner rig and furnace testing [2,3].

SEM micrographs of spall surfaces of the vendor 1 and vendor 3 EB-PVD coated specimens are presented in figures 8a and 8b. Note the columnar structure of the coatings that is thought to provide these coatings with superior strain tolerance. The coatings exhibit cracking through the columns parallel to the interface and appear to exhibit cracking along the columns perpendicular to the interface. Fractography of EB-PVD coated specimens tested in burner rigs has indicated that EB-PVD coatings spall by cracking along the bond coat/top coat interface, generally with a complete loss of the top coat in the spall region [7]. However, all of the EB-PVD coatings tested in this study showed a remnant of the top coat adhering to the bond coat in the spall region (figure 8). This may be a result of high stresses in the ceramic, away from the top coat/bond coat interface, generated by the severe thermal gradient through the top coat.

The results of testing to elucidate the effects of bond coat and top coat thickness, substrate type and substrate geometry are presented in figures 9a through 9d. There was a significant amount of scatter in the results for this portion of the testing. However, some limited conclusions can be drawn from the results.

Figure 9a clearly illustrates the longer life obtained for rod as compared to tube substrates. Two reasons for this life difference with substrate geometry are possible. First, an increase in life has been demonstrated for PS coatings deposited on substrates that are kept cool during deposition [8]. Therefore, coatings deposited on rods, which are better heat sinks than tubes, may exhibit longer lives than coatings deposited on tubes if the tubes are not adequately cooled during coating deposition. A second possibility is that the rods act as better heat sinks during testing and, therefore, exhbit lower temperatures and less expansion than the tubes. Lesser expansion may result in lower expansion mismatch stresses between the top and bond coats and, therefore, longer lives.

The results of testing tubes with varying thicknesses of ceramic top coat are presented in Figure 9b. The figure indicates poor durability of the 0.005cm thick coatings relative to the thicker coatings. While the chart also appears to indicate that 0.013cm thick coatings are better than thicker coatings, there is insufficient data to support this conclusion.

The data of figure 9c show the variation in life with thickness of bond coat. Again it is difficult to make specific conclusions as to the trend of the data. However, it appears that TBC life without a bond coat is less than the life with either a 0.010cm or a 0.018cm bond coat.

The results of testing to determine the effect of the substrate composition on the life of the coating are shown in figure 9d. The life of the coatings on the substrates of different composition could not be ranked at the 90% confidence level. The apparent ranking in increasing order, based only on the average lives, is: IN792, MAR-M 509, MAR-M 246, and B1900.

Surface roughness of the coating has been suggested to have an effect on the coating heating rate. Therefore, the surface roughness could also have an effect on the life of the coating. The vendor 10 ZrO_2-8wt.% Y_2O_3 coatings were purchased in the as-plasma-sprayed and the surface finished condition in order to examine the effect of coating roughness on coating life. Additionally, the roughness of all the samples tested in this study were measured to observe any general trends of roughness effects on the life of the coatings. The results did not show an apparent correlation of roughness to the life of the coatings.

A qualitative assessment of the effect of roughness on the heating rate of a coating was made by observing the time required after ignition to achieve visible heating of the coating. The observations were made from 400 frame/second film taken during testing. The data are plotted as hundredths of seconds versus coating roughness in figure 13. As expected, rougher coatings heated more quickly than smoother coatings.

Summary and Conclusions

Thermal barrier coating durability and protective capability in a high heat flux environment were examined using a H_2/O_2 rocket engine. A variety of vendor supplied TBCs as well as NASA applied TBCs were incorporated in the evaluation to provide a cross section of coating application processes. Several coatings showed potential for very long lives and most coatings provided excellent thermal protection during their pre-spall lifetime. In spite of excellent durability for some coatings, life reproducibility is a problem for TBCs under the severe conditions of this test. Examination of several coating parameters indicated that TBC life was a function of top coat chemistry and top

coat application process. TBC life was a strong function of processing differences between vendors (for a given coating chemistry) and the substrate geometry. TBC life appeared to be a weak function of bond coat thickness, top coat thickness and substrate composition. The surface roughness of the thermal barrier coatings had no discernible effect on coating life.

References

1. R. L. Dreshfield and R. A. Parr, "Application of Single Crystal Superalloys for Earth-to Orbit Propulsion Systems," NASA Technical Memorandum 89877 (1987).
2. R. A. Miller, "Current Status of Thermal Barrier Coatings - An Overview," Surf. Coating Tech. [30] 1-11 (1987).
3. T. E. Strangman, "Thermal Barrier Coatings for Turbine Airfoils," Thin Solid Films, 127, 93-105 (1985).
4. R. A. Miller and C. C. Berndt, "Performance of Thermal Barrier Coatings in High Heat Flux Environments," Thin Solid Films [119] 195-202 (1984).
5. R. J. Quentmeyer, H. J. Kasper and J. M. Kazaroff, "Investigation of the Effect of Ceramic Coatings on Rocket Thrust Chamber Life," AIAA Paper 78-1034 (NASA TM-78892).
6. J. A. Nesbitt and W. J. Brindley, "Thermal Analysis of Thermal Barrier Coatings in a High Heat Flux Environment," Proc. 1988 Conference on Earth-to-Orbit Propulsion Technology, Marshall Space Flight Center, Huntsville, Al., May 10-12, 1988.
7. T. E. Strangman, J. Neuman and A. Liu, "Thermal Barrier Coating Life-Prediction Model Development," NASA CR-179648 (1987).
8. J. W. Watson and S. R. Levine, "Depostion Stress Effects on the Life of Thermal Barrier Coatings on Burner Rigs," Thin Solid Films, 119, 185-193 (1984).

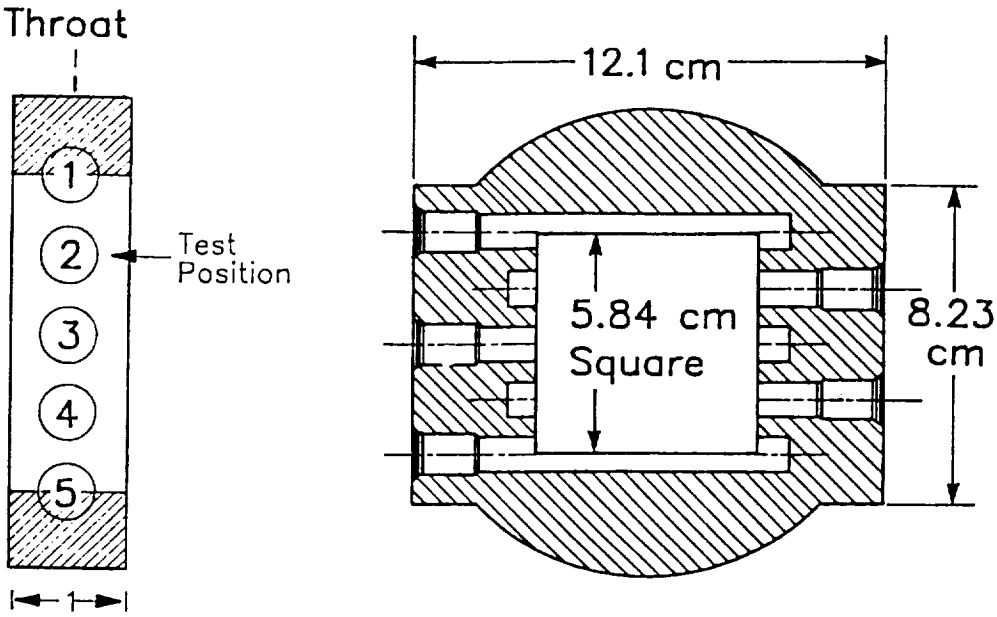

Figure 1. Schematic of sample holder. All samples were tested in the indicated position.

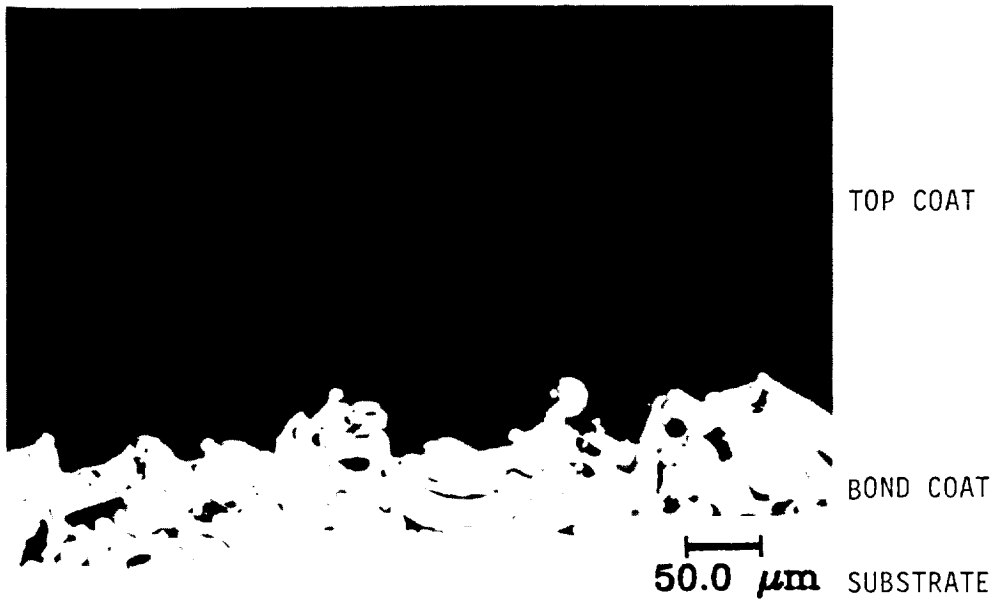

Figure 2. Optical micrograph of a cross sectioned, plasma sprayed, NASA-LeRC two layer thermal barrier coating.

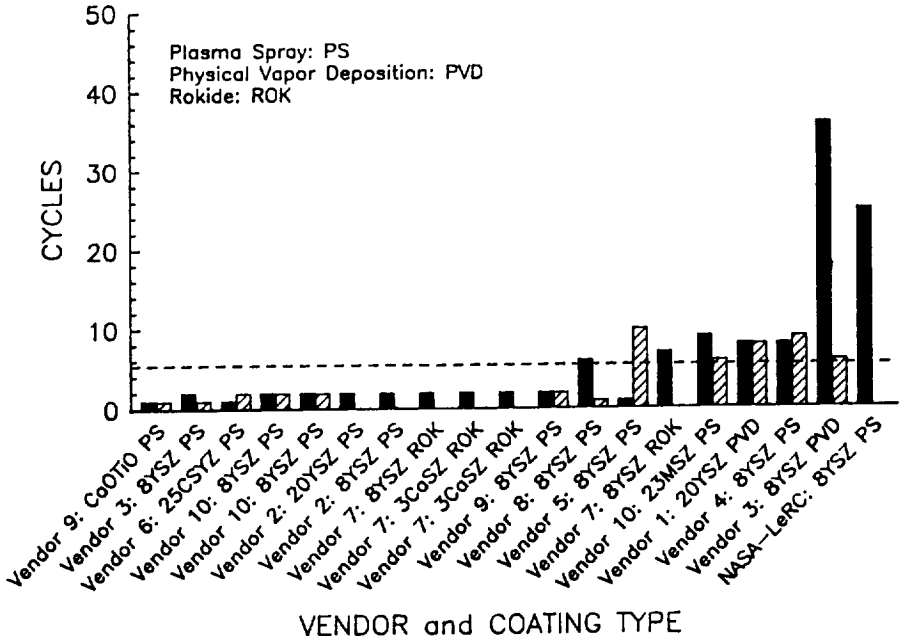

Figure 3. Histogram of cyclic life to the first observation of spallation of coatings applied to tube substrates. The dashed line indicates the "average" life.

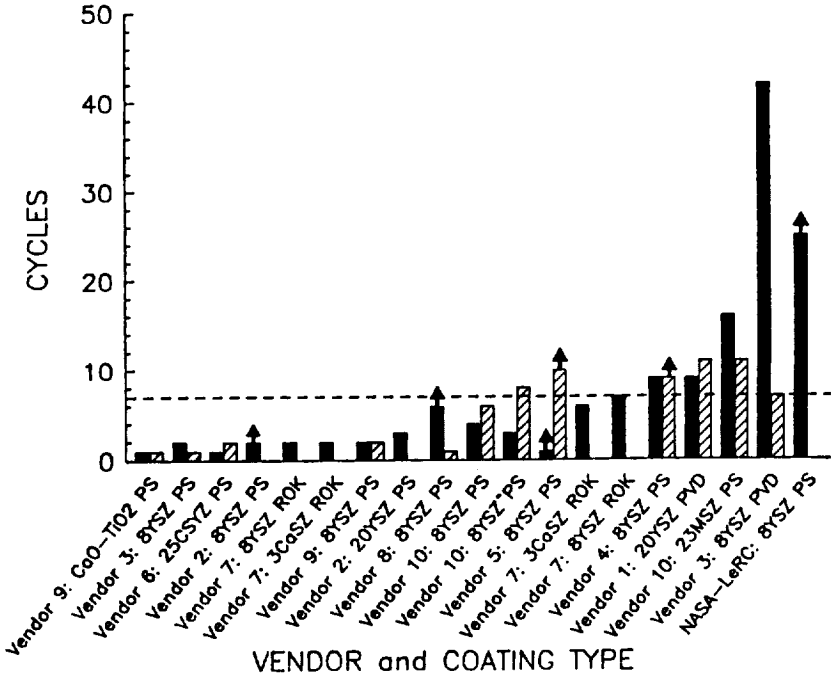

Figure 4. Histogram of cyclic life to substrate melting of coatings applied to tube substrates. Arrows indicate samples that did not fail at the applied cycles. The dashed line indicates the "average" life.

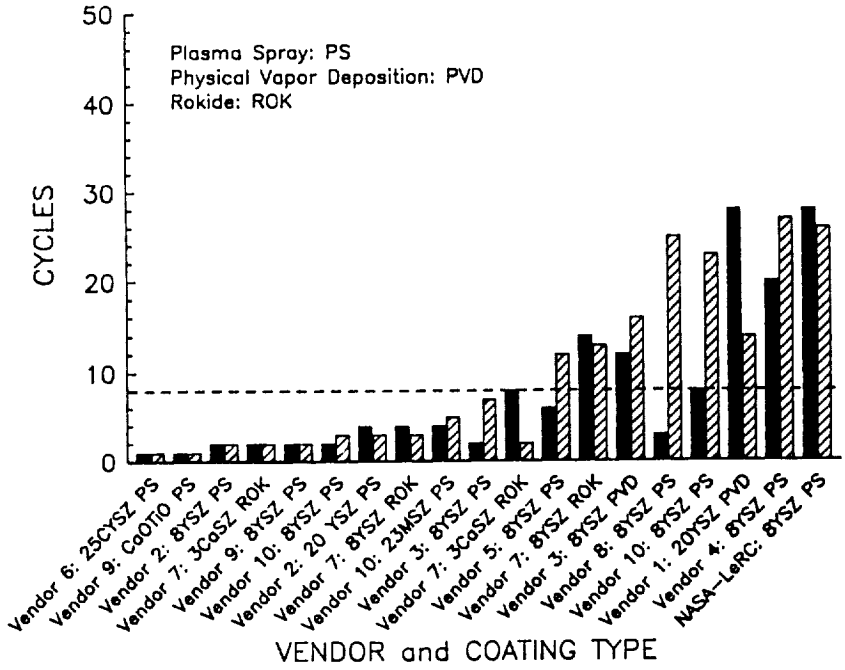

Figure 5. Histogram of cyclic life to the first observation of spallation of coatings applied to rod substrates. The dashed line indicates the "average" life.

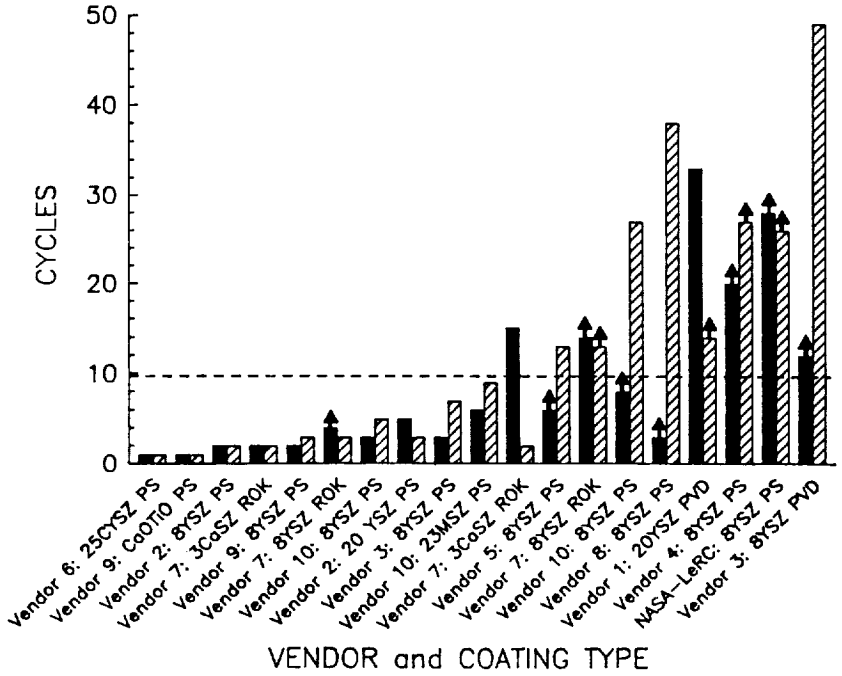

Figure 6. Histogram of cyclic life to substrate melting of coatings applied to rod substrates. Arrows indicate samples samples that did not fail at the applies cycles. The dashed line indicates the "average" life.

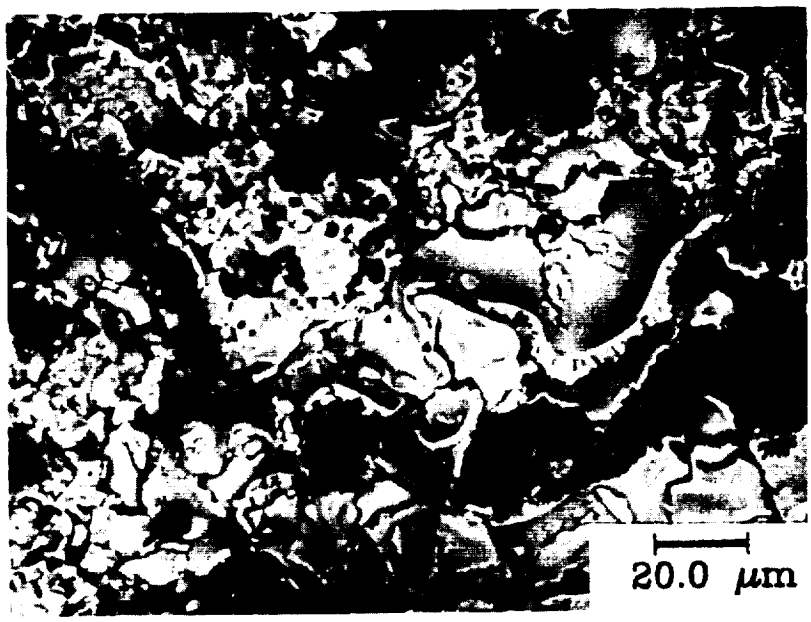

(a)

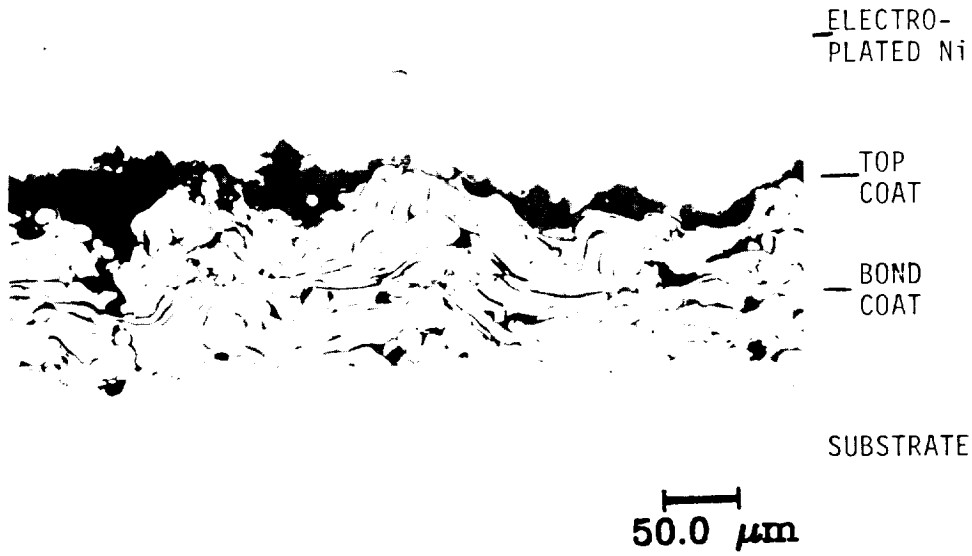

(b)

Figure 7. (a) SEM micrograph of the spalled surface of a NASA-LeRC plasma sprayed TBC. The light areas are ZrO_2 top coat and the dark areas are bond coat. (b) Optical micrograph of a cross sectioned NASA-LeRC TBC tested to spallation. Electroplated Ni layer was added after testing to aid in metallographic preparation.

(a)

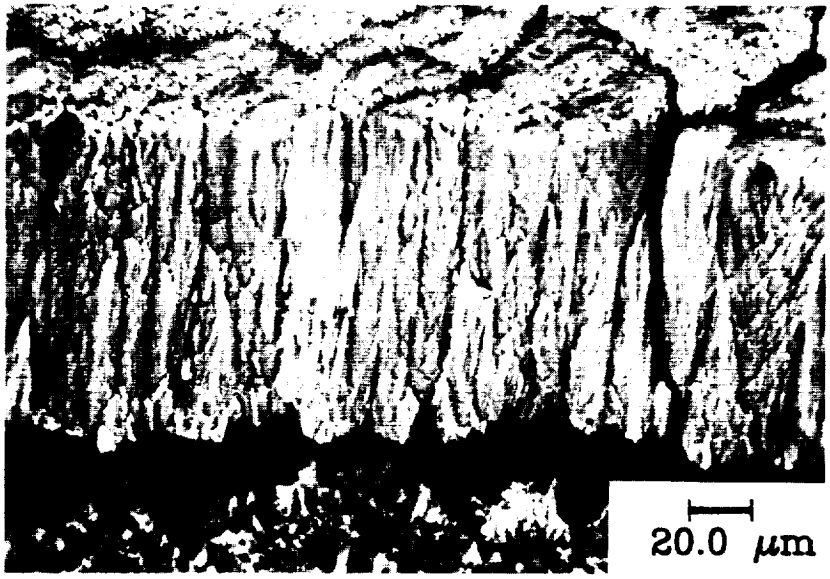

(b)

Figure 8. SEM micrographs of spalled surfaces of (a) the vendor 1 EB-PVD coating and (b) of the vendor 3 EB-PVD coating. The light areas are top coat and the dark areas are bond coat.

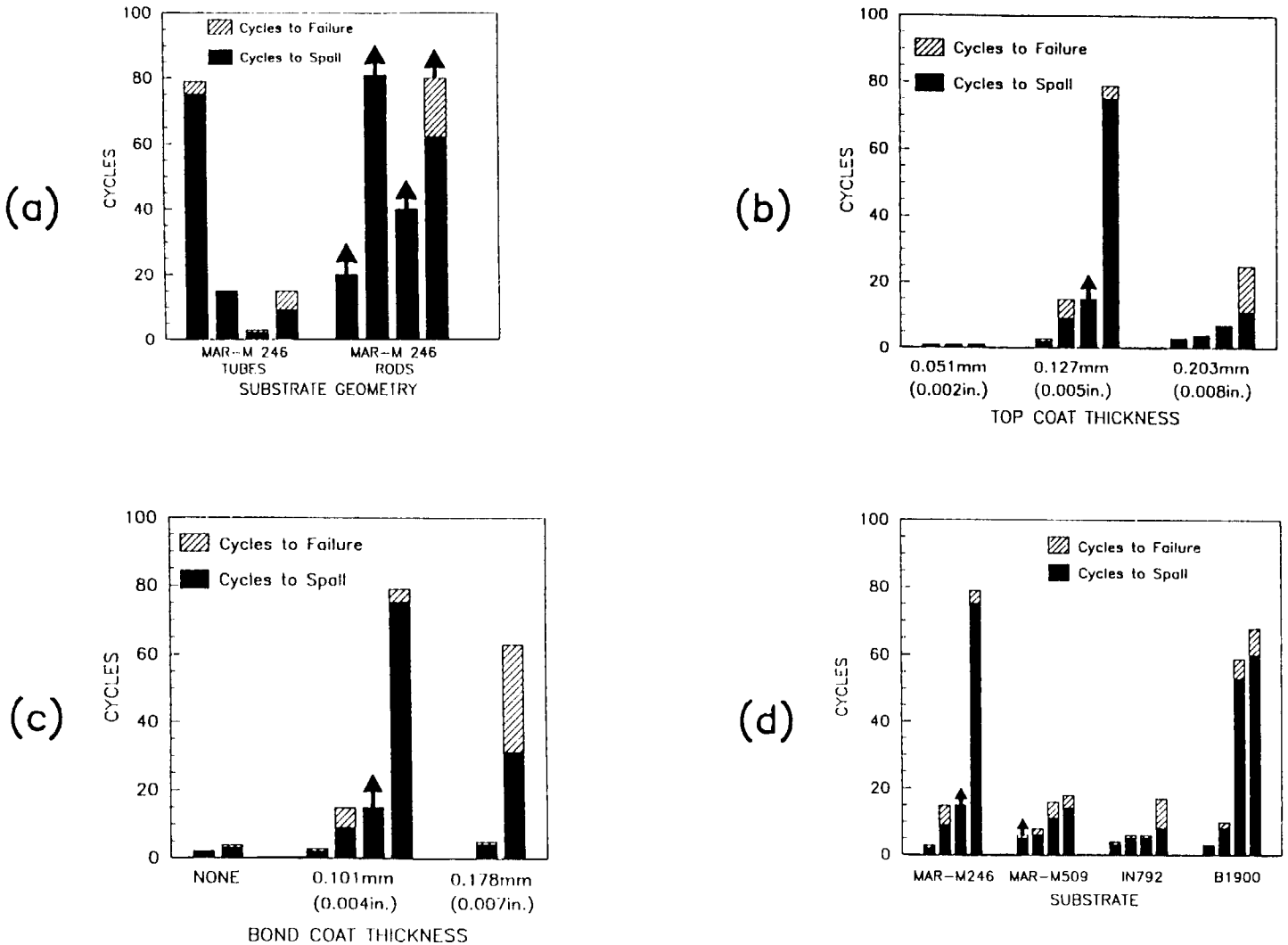

Figure 9. Cyclic life for coatings with: (a) differing substrate geometries, (b) differing top coat thicknesses, (c) differing substrate compositions and (d) differing bond coat thicknesses. The arrows indicate samples that have not failed at the applied cycles.

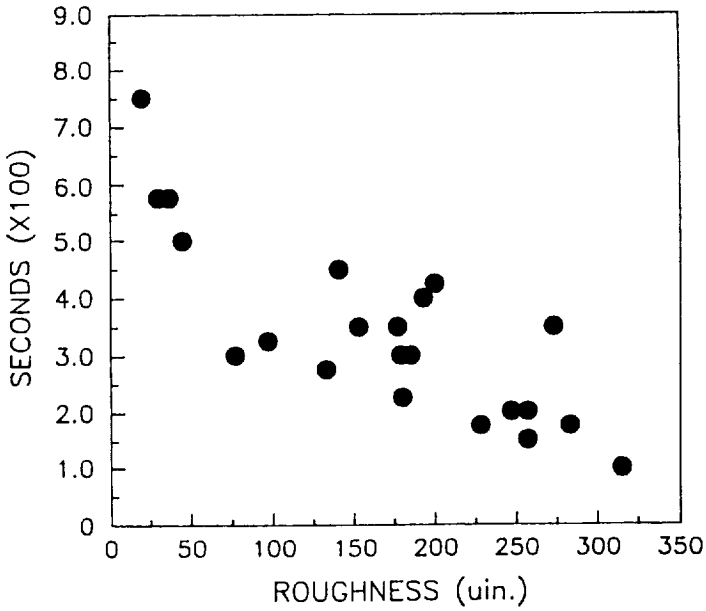

Figure 10. Elapsed time (from ignition to visible heating) versus top coat surface roughness.